Time and dose-dependent antimicrobial potential of Ag nanoparticles synthesized by top-down approach

Dhermendra K. Tiwari[1], J. Behari[1,*] and P. Sen[2]

[1]School of Environmental Science, and
[2]School of Physical Science, Jawaharlal Nehru University, New Delhi 110 067, India

Silver nanoparticles are known to be good antibiotic agents. In this study, silver (Ag) nanoparticles (~6 nm) were synthesized using electro-exploding wire (EEW) technique. Antibacterial action of Ag nanoparticles was studied both in liquid and solid phase using colony-forming unit (CFU) detection. Time and dose-dependent study of Ag nanoparticles shows that the effectiveness of particles increases with increasing particle dose and treatment time. This effect was dose-dependent and more pronounced against Gram-negative bacteria compared to Gram-positive bacteria. Transmission electron microscopy result shows particle binding with bacterial cell membrane. Membrane potential assay and cytoplasm diffusion assay show the effectiveness of Ag nanoparticle used in this study.

Keywords: Antimicrobial potential, colony-forming unit, nanoparticles, ultrasonic irradiation.

AMONG the inorganic antibacterial agents, silver (Ag) has been known most extensively since ancient times to fight infections and control spoilage. The antibacterial and antiviral actions of Ag, Ag^+ and Ag compounds have been thoroughly investigated[1–3]. It is well known that silver ion and silver-based compounds are highly toxic to microorganisms[4], showing strong biocidal effect against as many as 16 species of bacteria, including *Escherichia coli*[5]. However, Ag^+ ions or salts have only limited usefulness as antimicrobial agents for several reasons: interfering effects of salts and the antimicrobial mechanism of continuous release of enough concentration of Ag ion from the metal form. In contrast, these kinds of limitation can be overcome using Ag nanoparticles.

Nanoparticles are highly reactive species because of large surface area. Ag nanoparticles have been tested in various fields of biological sciences, viz. drug delivery, wound treatment, binding with HIV gp120 protein[6], in water treatment and as an antibacterial compound against both Gram-positive and Gram-negative bacteria[7–13]. Most of the bacteria have developed resistance to antibiotics. Thus there is a future need to develop a substitute for antibiotics[9]. Ag nanoparticles are attractive as these are non-toxic to the human body at low concentration and have broad-spectrum antibacterial nature. Ag nanoparticles inhibit bacterial growth at a low concentration than antibiotics and have no side effects[10]. Silver nanoparticle has the capability to kill living contaminants[14] present in wastewater as well as permanently bind to the filter membrane[7].

Size and stability are important factors for the biocidal nature of Ag nanoparticles. We have synthesized small size Ag nanoparticles by an approach that avoids other salt and chemical contaminants emerging out in the chemical synthesis of these Ag nanoparticles.

Ag nanoparticles were prepared according to method adopted by Siwach and Sen[15]. These were synthesized by employing a novel, physical, top-down approach of EEW (electro exploding wire) technique. In this technique, a wire is exploded on a plate of the same material by passing a current of 10^{10} A/m^2, in a time of 10^{-6} s. Flow of current through the wire–plate leads to heating at the point of contact, followed by melting. The melted metal at the point of contact is further heated by the ever-increasing current density due to increase in resistance, which leads to evaporation of material and subsequent plasma formation. This plasma is contained by the self-induced magnetic field. When the vapour pressure of the plasma overwhelms the self-induced magnetic field, explosion occurs and the plasma products are dispersed in the medium with high speed. Silver nanoparticles are thus synthesized by fragmentation of the parent material in water medium, which simultaneously caps and collects the particles. Synthesized Ag nanoparticles are free from extraneous impurities, as no chemicals are used in the process of synthesis. Parameters like current density, material type, wire dimension and the medium in which explosion is carried out are monitored to have control over the entire process of exploding the wire[16,17].

E. coli DH5α and *Bacillus subtilis* were grown overnight in Luria Bertani (LB) broth at 37°C. Bacterial cells were centrifuged at 6000 rpm for 15 min; washed cell pellets were resuspended in LB and optical density (OD) was adjusted to 0.1 at 595 nm.

The synthesized nanoparticles were characterized using X-ray diffraction (XRD) and transmission electron microscopy (TEM) techniques. TEM images were observed with a JEOL-2010F, UHR, TEM, operating at 200 kV. Samples were prepared by placing a drop of homogeneous suspension on a copper grid with a lacey carbon film and allowing it to dry in air. After ultrasonication for 10 min, XRD patterns were recorded on Bruker D8 advance diffractometer[15] using CuKα radiation (λ = 1.5418).

The bactericidal activity of Ag nanoparticle was checked by determining the MIC (minimum inhibitory concentration). Minimal concentration of Ag nanoparticles which inhibits the growth of *E. coli* DH5α and *B. subtilis* is known as MIC. Bacterial cells were grown in LB medium and 500 µl of 24-h-old bacterial culture (0.1 OD) was spreaded over the LB agar plates, supplemented with 10, 20, 40, 50 and 80 µg/ml of bared Ag nanoparticles. All

*For correspondence. (e-mail: jbehari2000@yahoo.co.in)

plates were incubated in BOD incubator for 24 h. Antimicrobial test compound below the MIC cannot inhibit microbial growth.

The Ag nanoparticles were suspended in triple distilled water to conduct the time-dependent antibacterial study. *E. coli* DH5α and *B. subtilis* cells were treated with 2.0 ml of each concentration (0, 10, 20, 30, 40, 50, 60, 70, 80, 90 and 100 μg/ml) of Ag nanoparticle for 30 min as well as with varying time intervals for each concentration (30 min, 2, 6 and 12 h). Before using the Ag nanoparticle, the suspension was homogenized using an ultrasonic cleaner. Each treated bacterial culture was serially diluted till 10^6 dilution factor and 100 μl from each culture was homogeneously spread in LB agar plates. All plates were incubated at 37°C for 24 h and the number of colonies grown on agar plate was counted.

Growth pattern of *E. coli* DH5α and *B. subtilis* was studied with 0, 10, 25, 35 μg/ml and 0, 15, 35, 55, 85 μg/ml concentration of homogenized Ag nanoparticle simultaneously. *E. coli* DH5α and *B. subtilis* cells (OD 0.1) were treated for 1 h, with varying concentrations of Ag nanoparticle as mentioned above and inoculated in 200 ml of Erlenmeyer necked flask. All the flasks were put on rotatory shaker (180 rpm) at 37°C. Untreated culture flask was used as control. Optical density was measured after every hour (up to 20 h) using UV–visible spectrophotometer at 595 nm.

Zone of inhibition test was performed in LB agar plates supplemented with 20 μg/ml of Ag nanoparticle. For this, 20 ml LB agar was poured in well-rinsed, autoclaved petri plates, 1.0 ml of active bacterial culture was homogeneously spread in the agar plates and 500 μl of Ag-nanoparticle solution filled in deep blocks, prepared by cutting the agar by gel puncture. The plates were incubated at 37°C for 24 h. The zone size was determined by measuring the radius of the zone. The test performed with high concentration of Ag nanoparticles did not show a large zone of inhibition because particles had settled at the bottom.

To examine the interaction of Ag nanoparticles with bacterial strains, cells were grown in liquid LB medium at 35 ± 2°C for 24 h. Growing cells were centrifuged and mixed in phosphate buffer saline (PBS). Then 1.0 ml of bacterial solution was mixed in 1.0 ml of Ag-nanoparticle solution (40 μg/ml) and incubated for 4 h. Interaction of Ag nanoparticles with bacterial cells was studied by TEM. The effect of Ag nanoparticles on the bacterial cells was monitored by depositing 10 μg of each sample on carbon-coated copper TEM grids followed by air-drying. TEM image of *E. coli* cells was analysed by a Hitachi FEI Philips Morgagni 268D TEM instrument operating at an accelerating voltage of 100 kV.

Bacterial cells (1.0 ml) were treated with 1.0 ml of Ag-nanoparticle solution in the concentrations 15, 25, 35, 45, 55, 65 and 75 μg/ml. At the same time all the samples were exposed for 5 and 15 min at 35 kHz ultrasound frequency. After 30 min of treatment, 100 μl *E. coli* DH5α solution was spread over the LB agar plates. All petri plates were incubated at 37°C for 24 h. Colony number was counted by a colony counter. In an effort to eliminate errors in the procedure, all assays were carried out in duplicates. Dilution experiment was performed in 48 well-brushed plates at 37°C.

Cytoplasm leakage analysis for Ag nanoparticle-treated cells was done as follows. *E. coli* DH5α and *B. subtilis* cells were treated with Ag nanoparticles. Treated cells were centrifuged and supernatant used to study protein, nucleic acid and K^+ ion leakage analysis.

For the nucleic acid leakage test, the amount of nucleic acid released in 5, 15, 35, 45, 55, 65, 75, 95, 115 and 200 μg/ml Ag nanoparticle-treated cells was measured at 260 nm (A_{260}) using UV–visible spectrophotometer. For preliminary identification of nucleic acid leakage, ninhydrin test showed positive result. The experiment was repeated for minimizing error.

Protein leakage analysis was performed using Bradford assay. Bacterial cells of *E. coli* DH5α and *B. subtilis* were treated with 10, 30, 50 and 100 μg/ml Ag-nanoparticle solution for 1 h and 4 h. Supernatant was collected after centrifugation (at 6000 rpm) for 15 min. For each sample, 200 μl of the supernatant was mixed in 800 μl of Bradford reagent. Optical density (at 595 nm) was measured after 10 min of incubation in the dark. BSA was used as a standard protein.

If the Ag nanoparticle disrupts the bacterial cells, the concentration of K^+ will increase in the extracellular fluid due to leakage of intracellular material. The K^+ ion concentration will also increase in the extracellular fluid as the concentration of nanoparticle increases. Active culture of *E. coli* DH5α and *B. subtilis* cells was treated with 25, 50, 100, 200, 400 and 600 μg/ml of Ag-nanoparticle solution for 2 h. Treated samples were centrifuged for 15 min at 5000 rpm, and the supernatant was stored for determination of K^+ by atomic absorption spectroscopy. Multivalent ion standard used for this assay was purchased from Sigma-Aldrich, India.

SDS (sodium dodecyl sulphate) is a detergent which destroys bacterial cells by disrupting the cell membrane. If the bacterial cells lose membrane stability due to any stress effect, SDS will disrupt these cells more effectively than the normal cells. The effect of Ag nanoparticles on the outer membrane of the bacteria was checked by SDS treatment of pre-treated cells (with Ag nanoparticle) of *E. coli* DH5α and *B. subtilis*. Active culture of *E. coli* and *B. subtilis* was mixed in PBS-buffer containing 35 μg/ml Ag nanoparticle and incubated for 30 min. Cells were centrifuged and the pellet mixed in the same volume of PBS. SDS (0.15%) was mixed in Ag nanoparticle-treated cells. OD was measured after every 2 min time interval.

XRD and TEM results of Ag nanoparticles used in this study are shown in Figures 1 and 2. Figure 1 shows XRD data of the Ag nanoparticles. The peaks at $2\theta = 38.14°$,

44.34°, 64.54° and 77.47° can be assigned to reflections from the (1 1 1), (2 0 0), (2 2 0) and (3 1 1) planes respectively, of metallic silver in FCC phase. Figure 2 *a* shows a representative TEM image of a large number of Ag nanoparticles at a magnification of 30,000. Though it appears that the size of such particles is in the range 10 nm or larger, we believe that these larger particles are composed of van der Waals clusters of smaller entities. To demonstrate this we show in Figure 2 *b*, a high-resolution image (magnification = 800,000) of two almost spherical particles joined in the middle. From geometry, it is clear that these individual particles are 6–7 nm in diameter, while the composite particle in lower resolution would appear to be in the range 20 nm. The high-resolution TEM data show crystal planes and this further supports XRD analysis for the crystalline nature of Ag nanoparticles.

Figures 3 and 4 show the growth of *E. coli* DH5α and *B. subtilis*. The growth of the former is inhibited at a concentration of less than 10 μg/ml (Figure 3). This is the minimum concentration of the nanoparticle when the growth of *E. coli* DH5α is inhibited, i.e. MIC of Ag nanoparticle. Figure 4 shows the growth inhibition of *B. subtilis*. *B. subtilis* is inhibited at the same concentration of Ag nanoparticle but the rate of inhibition appears to be slow with increasing concentration compared to *E. coli*. It is suggested that the MIC of *B. subtilis* is higher than *E. coli* DH5α. The mechanism by which the nanoparticles are able to inhibit bacterial growth is not well understood, but it is suggested that the Ag nanoparticle affects the membrane of both the bacterial strains. It may lead to significant increase in the permeability and affect membrane transport[18].

Let us now consider the time-dependent treatment of bacterial strains. All the treated bacterial samples were homogeneously spread on LB agar plates. The number of colonies decreased as concentration increased in both *E. coli* DH5α as well as *B. subtilis* and 60% inhibition was observed at 50 μg/ml concentration (30 min treatment). When treatment time was increased from 30 min to 6 h, 10 μg/ml Ag nanoparticle was sufficient to inhibit 60% bacterial growth (Figure 5) and 50 μg/ml was sufficient to cause 100% inhibition.

On the other hand, when nanoparticles were spread homogeneously on the agar plate followed by 100 μl culture (OD 0.1), it was found that the number of colonies was less than that calculated in the procedure mentioned above. It is concluded that the culture treated in liquid

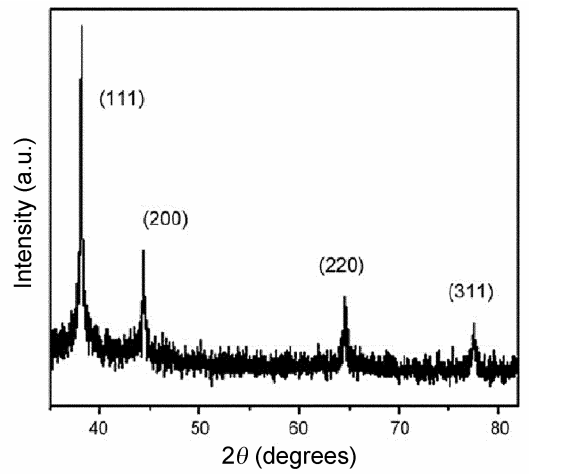

Figure 1. XRD pattern of Ag nanoparticles employed in the study.

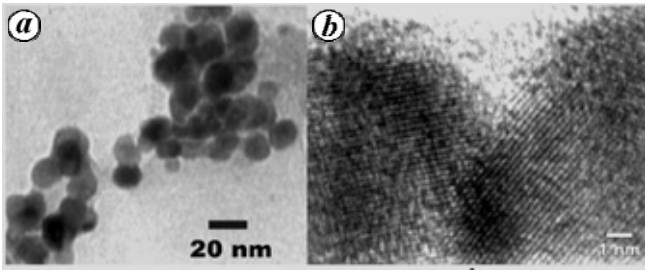

Figure 2. ***a***, TEM image of a large collection of nanoparticles. ***b***, Higher magnification from a selected region showing van der Waals cluster[15] of two particles, each about 6 nm across.

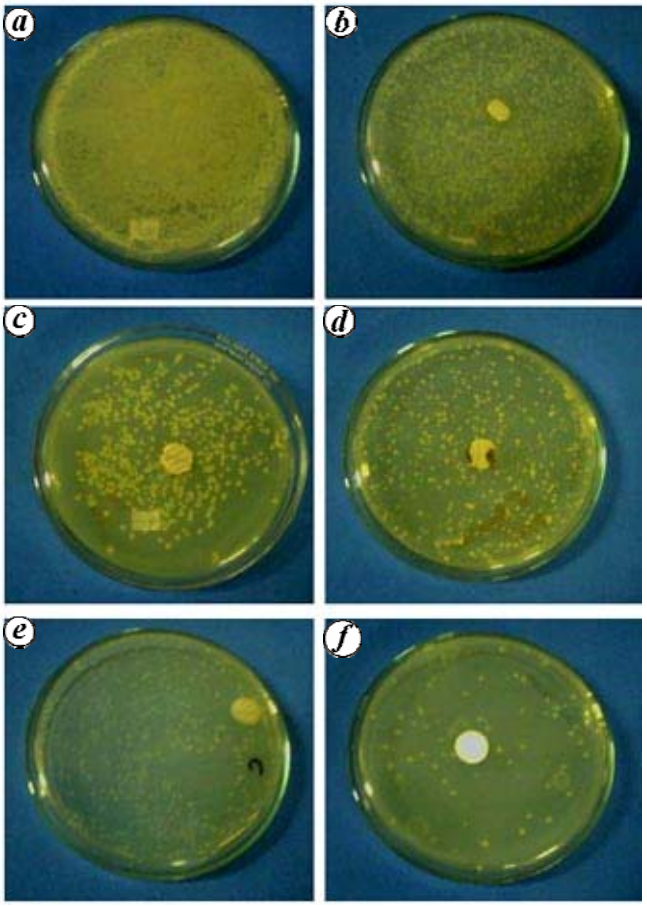

Figure 3. MIC test for *Escherichia coli*. (***a***) Control. ***b***–***f***, Plate supplemented with (***b***) 10 μg/ml, (***c***) 20 μg/ml, (***d***) 40 μg/ml, (***e***) 50 μg/ml and (***f***) 80 μg/ml of Ag nanoparticles.

phase is more effective because of the greater chances of bacteria–nanoparticles interaction.

In contrast, Ag nanoparticle was found to have less significant effect on the growth of Gram-positive *B. subtilis* (Figure 6). Less reduction in bacterial growth was observed till the concentration of Ag nanoparticle increased to 30 μg/ml (2 h treated culture). A concentration of 30 μg/ml was sufficient to inhibit 60% bacterial growth after 6 h treatment; it was 85% after 12 h of treatment (Figure 6). No growth was found when the culture was treated with 90 μg/ml of Ag nanoparticle for a short time (30 min). As the time of treatment increased, 50 μg/ml of particle concentration was sufficient for complete inhibition of growth. It was observed that when volume of the medium was high, the particles settled at the bottom and the chances of particle-bacterial cell interaction were reduced. It has been reported that the positive charge on Ag ion is an important factor for its antibacterial nature, through electrostatic interaction between the negatively charged cell membrane of the microorganisms and positively charged nanoparticles[19–21]. It is proposed that the electrostatic force might be an additional cause for the interaction of the nanoparticles with the bacteria[22].

Figures 7 and 8 show the effect of Ag nanoparticle on the growth of *E. coli* DH5α and *B. subtilis*, where time-dependent changes in bacterial growth are monitored by measuring OD at 595 nm (OD_{595}). The measurement of OD was carried out at 595 nm to avoid strong absorption due to the Ag nanoparticle in the region 380–450 nm and from bacterial cellular components such as nucleic acids (A_{260}), proteins (A_{280}) and molecules present in the LB

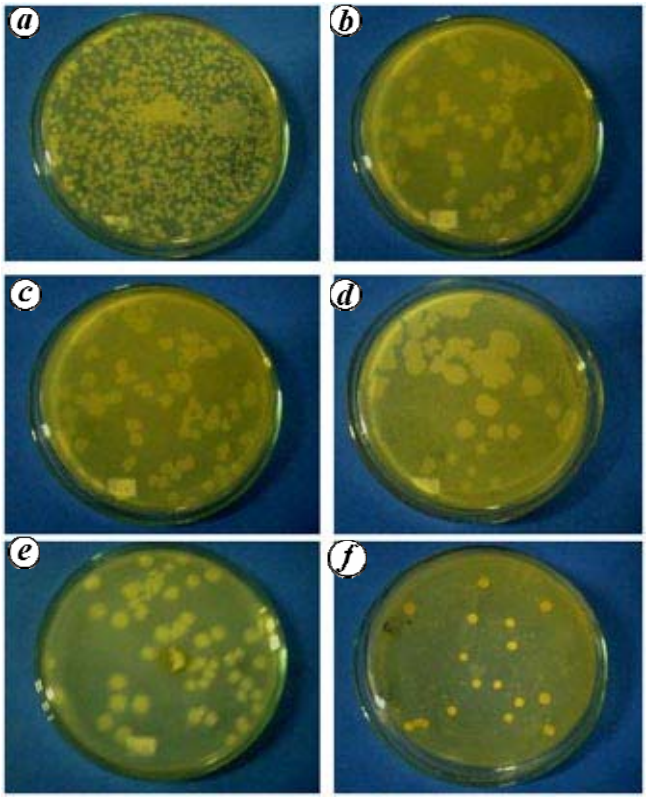

Figure 4. MIC test for *Bacillus subtilis*. (***a***) Control. ***b–f***, Plate supplemented with (***b***) 10 μg/ml, (***c***) 20 μg/ml, (***d***) 40 μg/ml, (***e***) 50 μg/ml and (***f***) 80 μg/ml of Ag nanoparticles.

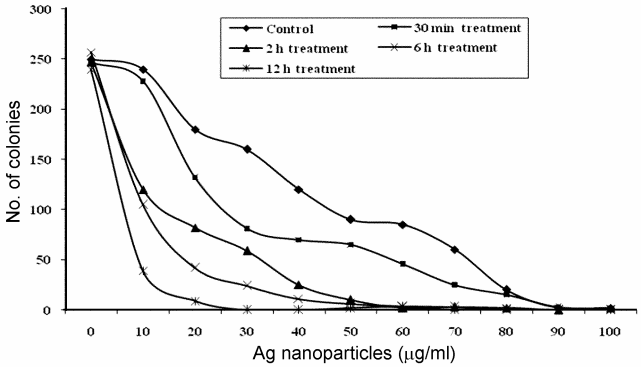

Figure 5. Viable number of cell counts of *E. coli* DH5α treated with Ag nanoparticle. The 24-h-old active culture of *E. coli* DH5α was treated for 30 min, 2, 6 and 12 h with various concentrations of Ag nanoparticle. Colony numbers were counted after 24 h of incubation.

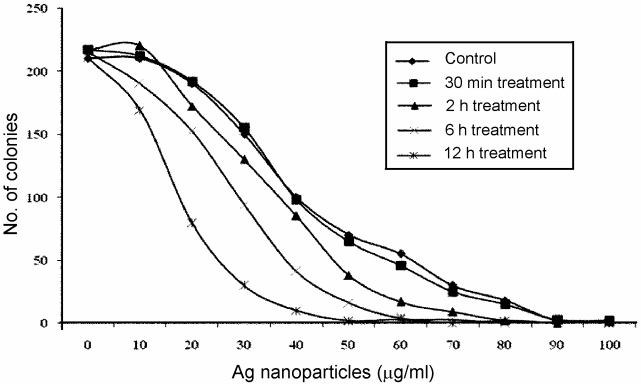

Figure 6. Viable number of cell counts of *B. subtilis* treated with Ag nanoparticle. The 24-h-old active culture of *B. subtilis* was treated for 30 min, 2, 6 and 12 h with various concentrations of Ag nanoparticle. Colony numbers were counted after 24 h of incubation.

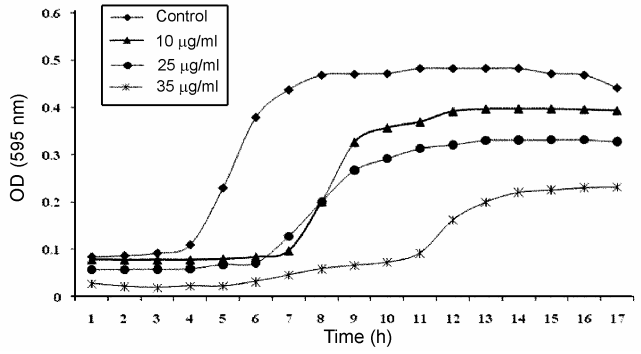

Figure 7. Growth curve of *E. coli* DH5α treated with Ag nanoparticle. Cells of *E. coli* DH5α were treated with 10, 25 and 35 μg/ml of Ag nanoparticle solution. OD of growing culture was measured at 1 h interval for 19 h.

medium such as sugar and carbohydrate that might absorb at $A_{400–500}$. The OD at 595 nm is due to the scattering of light by the bacterial cells. It is a function of bacterial cell density and thus correlates with the growth of the colonies. It is clear that Ag nanoparticle at a concentration 35 μg/ml inhibited growth of *E. coli* DH5α, whereas the effect was much less at this concentration in *B. subtilis*. Increasing concentration of Ag nanoparticle decreases the growth of *B. subtilis*, and the concentration at which growth stopped altogether was higher than that of *E. coli* DH5α (Figures 7 and 8).

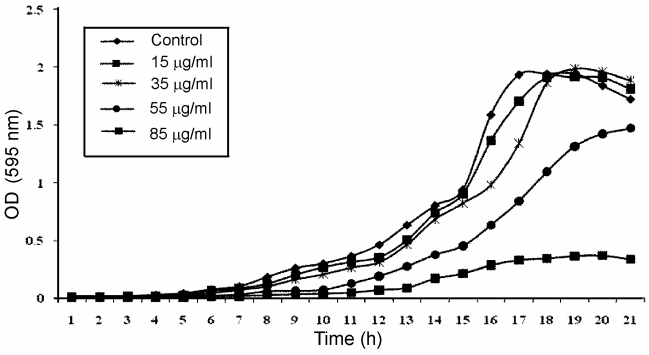

Figure 8. Growth curve of treated and non-treated *B. subtilis* strain. Cells of *B. subtilis* were treated with 15, 35, 55 and 85 μg/ml of Ag-nanoparticle solution. OD of growing culture was measured at 1 h interval for 21 h.

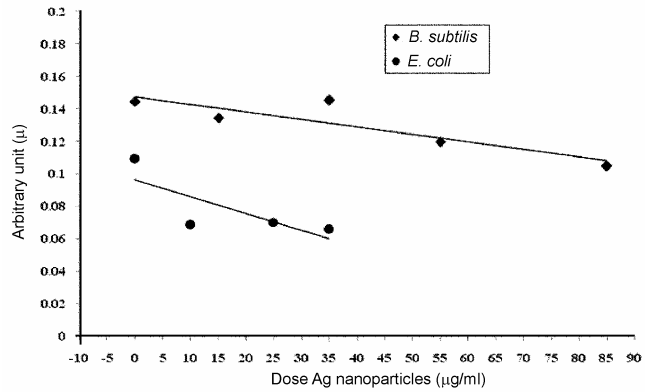

Figure 9. Effect of Ag nanoparticle on maximum growth rate constant (μ).

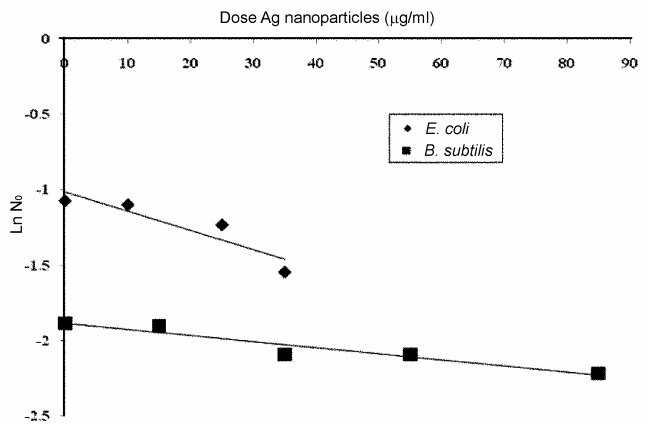

Figure 10. Effect of Ag nanoparticle on initial cell count (N_0).

Slope of the growth curve continuously decreased with increasing nanoparticle concentration, either from 0 to 35 μg/ml in *E. coli* DH5α or 0 to 85 μg/ml in *B. subtilis*. Growth dynamics of bacterial species is represented by the equation

$$\mu = 1/t \ln(N/N_0),$$

where N is the bacterial cell count at time t, N_0 the initial cell count and μ the growth rate constant for bacteria. Kinetic analysis for the growth of *E. coli* and *B. subtilis* indicates faster inhibition in Gram-negative bacteria. Figures 9 and 10 show that the slopes of trend lines representing the growth of *E. coli* are greater (faster inhibition) than *B. subtilis*.

Primarily Gram-positive and Gram-negative bacteria are categorized on the basis of cell-wall structure. Gram-negative bacteria contain a lipopolysaccharide layer at the exterior, followed underneath by a thin layer (7–8 nm) of peptidoglycan[23]. Lipopolysaccharides are not as rigid as peptidoglycan, because of the covalent linkage between the lipid and polysaccharide. Lipopolysaccharides contain negative charge[24], and attract the weak, positively charged Ag nanoparticle[25]. On the other hand, Gram-positve bacteria are principally composed of a thick layer (20–80 nm) of peptidoglycan, consisting of linear polysaccha-

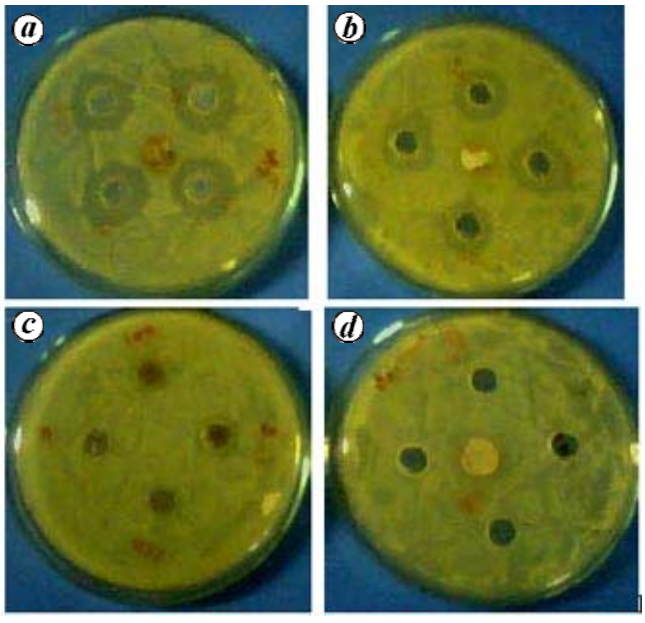

Figure 11. Zone of inhibition test for *E. coli* and *B. subtilis* against 20 μg/ml Ag nanoparticle solution. (***a***) *E. coli* with Ag nanoparticle, (***b***) *B. subtilis* with Ag nanoparticle, (***c***) Control *E. coli* and (***d***) Control *B. subtilis*.

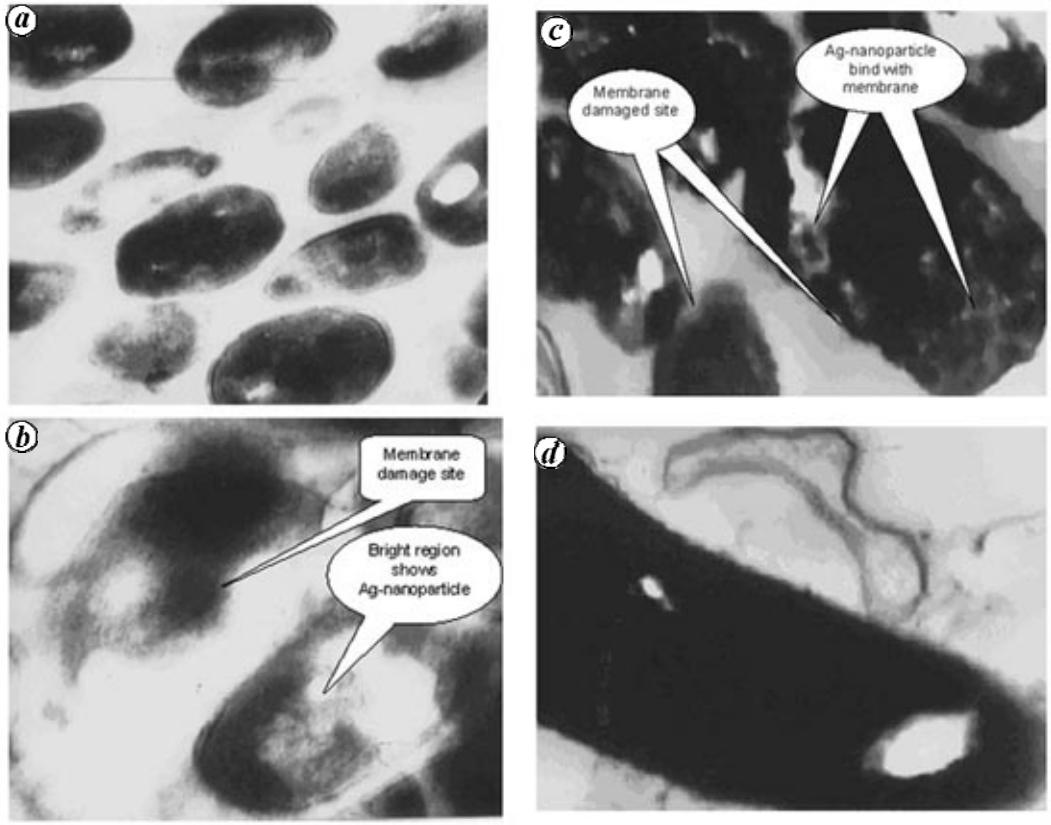

Figure 12. TEM images of *E. coli* cells. ***a***, Untreated *E. coli* (magnification 2650×). ***b***, *E. coli* grown on agar plates supplemented with Ag nanoparticle. Callous indicates particle attachment on membrane and partial membrane damage (magnification 11,500×). ***c***, *E. coli* treated with Ag particle (high magnification 11,500×). Callous indicates membrane damaged sites. Cells show damage at various sites. Ag nanoparticles appear on the cell surface. ***d***, Untreated *E. coli* (high magnification image at 11,500×).

ride chains cross-linked by short peptides to form a three-dimensional rigid structure[26]. The rigid and extended cross-linking not only endows the cell wall with fewer anchoring sites for the Ag nanoparticle, but also makes it difficult to penetrate. Thus Ag nanoparticles are more toxic to *E. coli* DH5α than *B. subtilis*.

Zone of inhibition test was done for identification of inhibition with 20 μg/ml Ag nanoparticle. It was found that 20 μg/ml concentration of Ag nanoparticle was able to inhibit bacterial growth and create a zone of 1.5 cm in *B. subtilis* and 3.1 cm in *E. coli* DH5α (Figure 11). We found that increasing the Ag-nanoparticle concentration did not show a consistent increase in the zone size in *B. subtilis* as well as in *E. coli* DH5α, because the nanoparticles settled at the bottom of the wells in the plates and the particle solution was not able to diffuse properly in the agar medium.

Interaction between Gram-negative *E. coli* and Ag nanoparticle is shown in the transmission electron photomicrographs (Figure 12). In a duration of bacterial cells with Ag nanoparticles, the particles appear on the bacterial surface. It is expected that the particle binds with the region rich in negatively charged functional groups. Longer incubation shows that the nanoparticles enter inside the bacterial cells (Figure 12 *c*). It is clear from Figure 12 *b* and *c* that the nanoparticles anchor the cell at several sites and cause damage at various sites in the membrane, which could result in cell lysis.

Ultrasonic waves are sound waves with frequency above 20 kHz. They increase the transport of small molecules in a liquid solution by increasing the convection in an otherwise stagnant or relatively slow-moving fluid[27–30]. In a pilot experiment we confirmed the inhibitory potential of ultrasonic waves by taking *E. coli* as an example (Figure 13).

From Figure 14, it is evident that the OD of the growing culture decreased when the cells were treated with both ultrasonic waves (35 kHz) and Ag nanoparticles. When the ultrasonic treatment was increased from 5 to 15 min, the growth of bacterial cells further decreased. Ultrasonic waves alone do not cause damage for 5 and 15 min exposure (Figure 13). Cells treated for 15 min had lesser OD than those treated for 5 min.

Ultrasonic waves can thus facilitate the entry of Ag nanoparticles and show enhanced antibacterial properties. It can be concluded from this investigation that not only

the binding of nanoparticle to the outer membrane is responsible for biocidal effect, but it is also caused due to binding of Ag nanoparticle with some intracellular components.

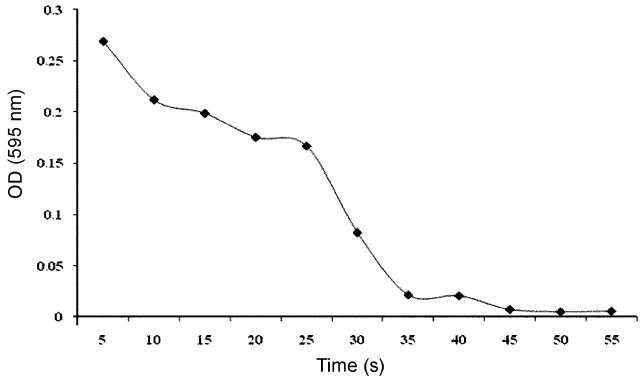

Figure 13. *E. coli* cells exposed to ultrasonic waves at 35 kHz frequency. No cell damage occurred till 15 min of ultrasonic treatment.

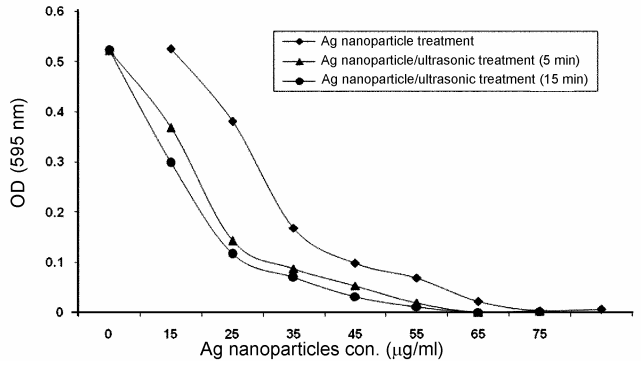

Figure 14. Growth of *E. coli* cells treated combined with ultrasonic waves and Ag nanoparticle. Cells of *E. coli* mixed in PBS buffer containing Ag nanoparticle were exposed to ultrasonic waves (35 kHz) for 5 and 15 min.

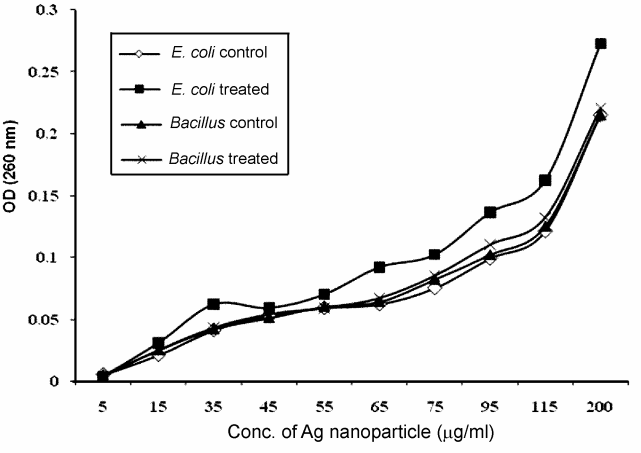

Figure 15. Bacterial cells treated with Ag nanoparticle. Supernatant of the treated cells shows presence of nucleic acid at A_{260}.

Ag nanoparticle injured cells have often been reported to release ninhydrin-positive materials, purine and pyrimidine into a suspension. Nucleic acid and its relative compounds such as pyrimidine and purine are well known to absorb UV light at 260 nm range. The presence of these materials in a suspension indicates damage to the cells at the membrane level.

The amount of nucleic acid released into the suspension was analysed by measuring the absorbance at 260 nm. At the same concentration, the amount of nucleic acid released was higher in *E. coli* DH5α than *B. subtilis* (Figure 15). The amount of protein released in a suspension of the treated cells was estimated by Bradford assay (Figure 16). The amount of nucleic acid and protein released from the cells increased along with increasing concentration of Ag nanoparticles. However the leakage of nucleic acid and protein in *B. subtilis* was lower than the *E. coli* DH5α. These results indicate that most of the nanoparticle-treated cells were ghost cells from which intracellular material was released into the cell suspension. The antibacterial effect of Ag nanoparticle was severe in *E. coli* DH5α than *B. subtilis*.

Maintenance of membrane potential is an important factor for the survival and growth of bacteria. Membrane potential of *E. coli* DH5α and *B. subtilis* is largely maintained by a high intracellular K^+ ion concentration mediated by inward influx[31,32]. After the variable time-period of incubation of *E. coli* DH5α cells with Ag nanoparticle, it was found that the extracellular K^+ increased with increasing incubation period (Figure 17). Ag nanoparticle induced the massive loss of intracellular K^+ ion. The K^+ ion concentration in extracellular fluid indicates the extent of damage of bacterial cells by Ag nanoparticle. Increasing K^+ ion concentration indicates higher rate of cell damage (with increasing incubation time of bacterial cells in Ag nanoparticle environment).

The sensitivity of Ag nanoparticle-injured cells was measured by their capacity to be lysed by SDS. Cells in

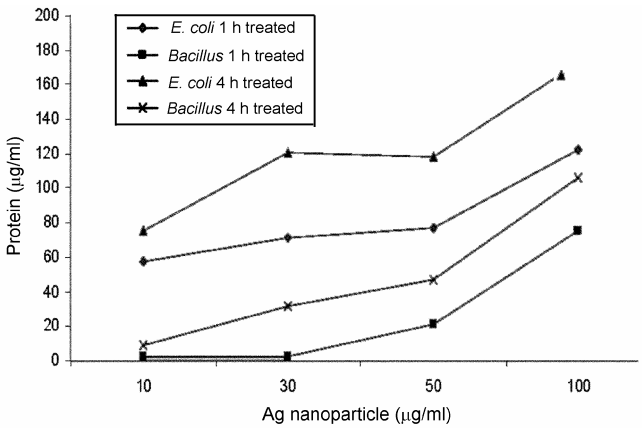

Figure 16. Bradford assay for protein leakage analysis of Ag nanoparticle-treated cells of *E. coli* and *B. subtilis* (1 h and 4 h treatment).

which the membrane deformed after treatment showed increased lasing effect. Nanoparticle-treated cells were mixed with PBS buffer and incubated at 37°C in a rotatory shaker (120 rpm) in the presence of 0.1% SDS, and cell density was measured at 600 nm (Figure 18). The OD of Ag nanoparticle-treated cells reduced dramatically within 30 min of incubation in the presence of SDS; but it did not decrease significantly in the absence of SDS. In untreated cell suspension, no significant decrease in OD was observed after 30 min, either in the presence or absence of Ag nanoparticles. The result validates the fact that most of the cells inactivated by Ag nanoparticle remain unlysed in cell suspension in the absence of SDS, and these are highly sensitive to lysis by SDS. It is clear from Figure 18 that the treatment of nanoparticles destabilizes the outer membrane. It is elucidated that the Ag nanoparticle can disrupt the outer membrane components such as porin and lipopolysaccharide[33]. On the other hand, *B. subtilis* is a Gram-positive bacteria. It does not have an outer membrane and the rate of cell destruction is less severe compared to *E. coli* DH5α. It is predicted that the Ag nanoparticles initially bind to outer membrane, but these particles can enter into the cells at higher concentration[22].

The present study shows the antibacterial effect of fine Ag nanoparticles (~6 nm) prepared using top-down approach. We have shown that the Ag nanoparticles causes antibacterial effect by rupturing the membrane of bacterial cells at low concentration. The concentration of nanoparticles is responsible for biocidal effect along with the treatment time. TEM image shows the particle binding and damage in cell wall of bacteria. Synergistic effect of nanoparticles along with ultrasonic treatment shows an enhanced antibacterial effect. This stems from the fact that ultrasonic waves expand the cell wall, which allows nanoparticles to enter into the cell. This also allows the nanoparticles to bind to the intracellular material, thereby causing antibacterial activity. From Figure 14 it is clear that the slope of the decay curve of Ag nanoparticle treatment is less compared to untrasonic treatment. Our findings substantiate the antibacterial nature of silver particles in the nano form.

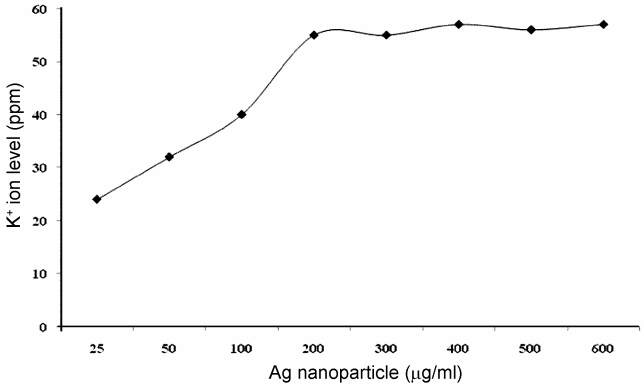

Figure 17. K^+ ion concentration measured by atomic absorption spectroscopy in the supernatant of *E. coli* DH5α cells treated with Ag nanoparticle.

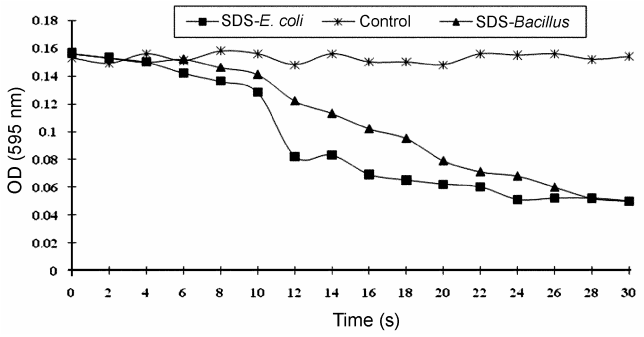

Figure 18. Membrane destabilization of the treated and non-treated cells of *E. coli* and *B. subtilis*. Ag-treated bacterial cells of *E. coli* and *B. subtilis* were incubated in sodium dodecyl sulphate (SDS) environment. OD was measured at 595 nm after 2 min interval, followed by 30 min.

1. Oka, M. T., Tomioka, Tomita, K., Nishino, A. and Ueda, S., Inactivation of enveloped viruses by a silver-thiosulfate complex. *Metal-based Drugs*, 1994, **1**, 511.
2. Oloffs, A., Crosse-Siestrup, C., Bisson, S., Rinck, M., Rudolvh, R. and Gross, U., Biocompatibility of silver-coated polyurethane catheters and silver-coated Dacron material. *Biomaterials*, 1994, **15**, 753–758.
3. Tokumaru, T., Shimizu, Y. and Fox, C. L., Antiviral activities of silver sulfadiazine and ocular infection. *Res. Commun. Chem. Pathol. Pharmacol*., 1984, **8**, 151–158.
4. Slawson, R. M., Van Dyke, M. I., Lee, H. and Trevors, J. T., Germanium and silver resistance, accumulation, and toxicity in microorganisms. *Plasmid*, 1992, **27**, 72–79.
5. Spadaro, J. A., Berger, T. J., Barranco, S. D., Chapin, S. E. and Becker, R. O, Antibacterial effects of silver electrodes with weak direct current. *Microb. Agents Chemother*., 1974, **6**, 637.
6. Elchiguuerra, J. L., Burt, J. L., Morones, J. R., Camacho-Bragado, A., Gao, X., Lara, H. H. and Yacaman, M. J., Interaction of silver nanoparticles with HIV-1. *J. Nanobiotechnol.*, 2005, **3**, 1477–3155.
7. Jain, P. and Pradeep, T., Potential of silver nanoparticle-coated polyurethane foam as an antibacterial water filter. *Biotechnol. Bioeng*., 2005, **90**, 59–63.
8. Son, W. K., Youk, J. H., Lee, T. S. and Park, W. H., Preparation of antimicrobial ultrafine cellulose acetate fibers with silver nanoparticles. *Macromol. Rapid Commun*., 2004, **25**, 1632–1637.
9. Li, P., Li, J., Wu, C., Wu, Q. and Li, J., Synergistic antibacterial effects of β-lactam antibiotic combined with silver nanoparticles. *Nanotechnology*, 2005, **16**, 1912–1917.
10. Lok, C. N. *et al.*, Proteomic analysis of the mode of antibacterial action of silver nanoparticles. *J. Proteo. Res.*, 2005, **5**, 916–924.
11. Baker, C., Pradhan, A., Pakstis, L., Pochan, D. J. and Shah, S. I., Synthesis and antibacterial properties of silver nanoparticles. *J. Nanosci. Nanotechnol*., 2005, **5**, 244–249.
12. Shrivastava, S., Bera, T., Roy, A., Singh, G., Ramachandran, P. and Das, D., Characterization of enhanced antibacterial effect of noval silver nanoparticle. *Nanotechnology*, 2007, **18**, 1–9.
13. Pal, S., Tak, Y. and Song, J. M., Does the antibacterial effect of silver nanoparticle depend on the shape of the nanoparticle? A study of the Gram-negative bacterium *Escherichia coli*. *Appl. Environ. Microbiol*., 2007, **73**, 1712–1720.

14. Gogoi, S. K., Gopinath, P., Paul, A., Ramesh, A., Ghosh, S. S. and Chattopadhyay, A., Green fluorescent protein expressing *E. coli* as a model system for investigating the antimicrobial activity of silver nanoparticle. *Langmuir*, 2006, **22**, 9322–9328.
15. Siwach, O. P. and Sen, P., Fluorescence properties of Ag nanoparticles in water. *Spectrochim. Acta, Part A*, 2008, **69**, 659–663.
16. Sen, P., Ghosh, J., Abdullah, A., Kumar, P. and Vandana, Preparation of Cu, Ag, Fe and Al nanoparticles by the exploding wire technique. *Proc. Indian Acad. Sci.* (*Chem. Sci.*), 2003, **115**, 499–508.
17. Goshwami, N. and Sen, P., Water-induced stabilization of ZnS nanoparticles. *Solid State Commun.*, 2004, **132**, 791–794.
18. Sondi, I. and Sondi, B. S., Silver nanoparticles as antimicrobial agent: A case study on *E. coli* as a model for Gram-negative bacteria. *J. Colloid Interface Sci*., 2004, **275**, 177–182.
19. Hamouda, T., Myc, A., Donovan, B., Shih, A., Reuter, J. D. and Baker, J. R., A novel surfactant nanoemulsion with a unique non-irritant topical antimicrobial activity against bacteria, enveloped virus and fungi. *Microbiol. Res.*, 2001, **156**, 1–7.
20. Dibrov, P., Dzioba, J., Gosink, K. K. and Hase, C. C., Chemiosmotic mechanism of antimicrobial activity of Ag(+) in *Vibrio cholera*. *Antimicrob. Agents Chemother*., 2002, **46**, 2668–2670.
21. Dragieva, I., Stoeva, S., Stoimenov, P., Pavlikianov, E. and Klabunde, K., Complex formation in solutions for chemical synthesis of nanoscaled particles prepared by borohydride reduction process. *Nanostruct. Mater*., 1999, **12**, 267–270.
22. Moron, J. R., Elechiguera, J. L., Ccamacho, A., Holt, K., Kouri, J. B., Ramirez, J. T. and Yachama, M., The bactericidal effect of silver nanoparticle. *Nanotechnology*, 2005, **16**, 2346–2353.
23. Madigan, M. and Martinko, J., *Brock Biology of Microorganisms*, Prentice Hall, NJ, 2005, 11th edn.
24. Salton, M. R. J., Kim, K. S. and Baron, S., *Medical Microbiology*, University of Texas Medical Branch, Galveston, 1996, 4th edn.
25. Sui, Z. M., Chen, X., Wang, L. Y., Xu, L. M., Zhuang, W. C., Chai, Y. C. and Yang, C. J., Capping effect of CTAB on positively charged Ag nanoparticles. *Physica E*, 2006, **33**, 308–314.
26. Baron, S., *Medical Microbiology*, University of Texas Medical Branch, Galveston, 1996, 4th edn.
27. Brennen, C. E., *Cavitation and Bubble Dynamics*, Oxford University Press, New York, 1995, p. 282.
28. Elder, S. A., Cavitation micro streaming. *J Acoust. Sci. Am.*, 1959, **31**, 54–64.
29. Nyborg, W. L., Ultrasonic microstreaming and related phenomena. *Br. J. Cancer*, 1982, **45**, 156–160.
30. Nyborg, W. L., Biological effect of ultrasound: Development of safety guidelines, Part II: General review. *Ultrasound Med. Biol*., 2001, **27**, 301–333.
31. Epstein, R. J., Stephens, J., Hanson, M., Chye, Y., Gossard, A. C., Petroff, P. M. and Awschalom, D. D., Voltage control of nuclear spin in ferromagnetic Schottky diodes. *Phys. Rev. B*, 2003, **68**, 1–4.
32. Lambert, M., Midy, P. and Desgrolard, P., Study of even-odd nuclei with N or $Z = 11°$ and 13°. *Phys. Rev. C*, 1973, **8**, 1728–1756.
33. Vaara, M., Agents that increase the permeability of the outer membrane. *Microbiol. Rev.*, 1992, **56**, 395–411.

Received 6 December 2007; revised accepted 30 July 2008

Coir geotextile-packed conduits for the removal of biodegradable matter from wastewater

A. Praveen[1,*], P. B. Sreelakshmy[2] and M. Gopan[3]

[1]Department of Civil Engineering, Government Rajiv Gandhi Institute of Technology, Pampady, Kottayam 686 501, India
[2]Department of Civil Engineering, Government Engineering College, Thrissur 680 009, India
[3]Kerala State Council for Science, Technology and Environment, Sasthra Bhavan, Thiruvananthapuram 695 001, India

Majority of residential units and small-scale commercial operators in India dispose wastewater either onsite or into the public drainage systems, without paying any attention to the public health and environmental impacts. Need for high investments and the requirement for large operational space are the reasons often quoted against the installation of a proper wastewater treatment unit. This communication presents a viable and cost-effective technology using coir geotextile, for the removal of organic matter from wastewater. Coir geotextile conduits, prepared using non-woven-type material and having a specific weight of 0.9–1.7 kg/m^2 could be an acceptable solution for most of the small-scale units.

Keywords: Biofilters, coir geotextiles, conduits, onsite disposal.

DESIGN and implementation of efficient wastewater treatment methods to meet the regional demands of pollution control have always been a major challenge facing the technologists. Several attempts in the past to limit uncontrolled discharges of polluted water have led to the development of wastewater-treatment solutions using innovative process concepts[1]. In spite of wide options being available for the choice of technology, the current approach in most developing countries is still to follow the conventional practices, without paying attention to better techniques and solutions. Among these, the most common method usually adopted by most of the residential or small-scale commercial units in India is either to discharge the wastewater onsite or drain it into any public wastewater carriage systems. It is also obvious that the setting up of conventional treatment systems for the above-mentioned situations may not be feasible due to the high cost of equipment and inadequate space for installation of these units. Also, setting up of a new, centralized wastewater treatment facility together with the laying of fresh sewer lines in emerging urban locations in India is certainly a cumbersome exercise. Under such circumstances, search for solutions that accommodate factors like cost-effectiveness in operation and low space requirement demands a more pragmatic approach in the

*For correspondence. (e-mail: arakkalpraveen@gmail.com)